Memory, Congruence, and Avalanche Events in Hysteretic Capillary Condensation

M. P. Lilly, P. T. Finley, and R. B. Hallock

Laboratory for Low Temperature Physics, Department of Physics and Astronomy, University of Massachusetts, Amherst, Massachusetts 01003

(Received 10 September 1993)

We report measurements of the hysteretic capillary condensation of helium in the porous material Nuclepore which display a hierarchy of return point memory effects and near congruence of closed internal hysteresis loops. Deviations from predictions based on the Preisach model of independent elementary hysteresis domains, originally developed to understand magnetic phenomena, are observed and are attributed to the appearance of additional domains on draining induced by the internal structure of the porous material. Pore intersections result in weak interactions among the pores which lead to avalanches.

PACS numbers: 67.70.+n, 47.55.Mh, 67.40.Hf, 68.45.Da

Hysteresis is a ubiquitous phenomenon, encountered in a wide variety of physical systems including magnetic materials, fluid invasion of porous beds, microfracturing of rock, martensitic transformations, charge density waves, adsorption of gases, etc. As an example of hysteretic behavior, capillary condensation has been widely studied, but a thorough understanding has been limited by the often complex geometry of the pore structure of the material. In an effort to study hysteresis, and, in particular, capillary condensation, in a simpler geometry, we have carried out experiments on the evolution of the hysteretic capillary condensation of superfluid helium into the nearly cylindrical pores of the filter material Nuclepore as the chemical potential is varied. We have chosen superfluid helium as the working fluid for these measurements due to the absence of viscosity and the existence of a mobile superfluid film resulting in rapid equilibration times.

Nuclepore [1], used in biomedical and other applications, is a thin polycarbonate sheet perforated by a high density of nearly cylindrical holes. The Nuclepore used in this study has a thickness of 10 μm and is threaded by $(3\times10^8)\pm15\%$ pores/cm^2 oriented at random within 34° of the normal to the plane of the Nuclepore. Each pore has a nominal diameter of 2000 Å $^{+0}_{-20}$%. Previous studies [2,3] have indicated that the pores have minimum diameter at the surface of the Nuclepore. Our simulations of the material indicate that the pores intersect; the most probable number of intersections per pore is about five and few pores suffer no intersections with others. The intersection region is apparently well defined with minimal extra volume present. Cluster simulations indicate that relatively few isolated clusters of disconnected pores exist in the material. Most pores participate in a macroscopic interconnected network and are apparently internally connected beyond the percolation threshold.

To conduct our experiments we measure the amount of helium adsorbed and capillary condensed in the Nuclepore as a function of the chemical potential of the helium (number of helium atoms present) at fixed temperature in a chamber located at the end of a standard cryostat insert. The technique [3] involves the measurement of the capacitance of the helium-Nuclepore sample as a function of the growing thickness of the helium film on the exposed surfaces as helium is added to the experimental chamber. The sample is made from a piece of Nuclepore as supplied from the manufacturer; 1000 Å thick Ag electrodes (1.9×1.9 cm^2) are evaporated directly on opposing faces of the Nuclepore in a vacuum evaporation apparatus. Scanning electron microscope studies of the resulting surfaces indicate that the Ag does not significantly interfere with the pore openings. To directly monitor the increase of helium chemical potential as helium is added to the experimental cell at fixed temperature, we monitor the velocity of third sound on a nearby glass substrate which is exposed to the same helium vapor pressure as is the Nuclepore sample. Third sound is a thickness and temperature wave which propagates on a thin superfluid helium film. The velocity of third sound is directly related to the local chemical potential [4]; the helium vapor in the cell is in equilibrium with the helium film. The third sound velocity allows us a simple *in situ* method to monitor changes in the chemical potential and ensure that we are able to reproduce chemical potential values in the apparatus.

To measure the capacitance and hence monitor the progress of the capillary condensation as helium is added to or withdrawn from the experimental chamber, we utilize a high precision capacitance bridge and are able to monitor changes in the capacitance to high resolution. To measure the third sound velocity we use time of flight techniques and measure the temperature fluctuation associated with the passage of a third sound pulse by use of a sensitive superconducting Al strip bolometer detector evaporated onto the glass substrate. Third sound is generated by the injection of a current pulse into an Ag film heater located ~1 cm away from the bolometer on the glass substrate. Thus, we readily measure the capacitance of the Nuclepore sample as a function of the third sound time of flight (chemical potential).

A typical experiment begins by bringing the (evacuated) experimental chamber to a selected operating temperature; here we choose $T=1.52$ K since at this temperature the third sound detector Al strip is maximally sensi-

0031-9007/93/71(25)/4186(4)$06.00

tive. Helium gas is slowly admitted to the experimental cell through a narrow capillary. We have checked to ensure that our results are independent of the rate [5] at which this is done. As helium is admitted to the cell, the chemical potential increases, the helium film thickness d increases, and the third sound time of flight τ increases; $\tau^2 \sim d^3$. At some point the chemical potential has increased enough so as to have caused all of the pores in the Nuclepore to capillary condense. Subsequent reduction in the chemical potential results in hysteretic behavior [3]. The resulting hysteresis loop shown in Fig. 1 is completely reproducible. Physically, the hysteresis results from the fact that the condensation and emptying events for a cylinder are caused by different instabilities [6]. As the chemical potential is increased, the thickness of the helium film which coats the flat surfaces and the interior surface of the cylindrical pores of the Nuclepore increases. As the radius of curvature of the surface of the film coating the interior of a pore shrinks, an instability develops which causes the pore to capillary condense due to a competition between the van der Waals and surface tension forces. The emptying of a pore takes place at a lower chemical potential than the original condensation since the controlling radius of curvature for the emptying is that created by the opening of the pore rather than that created by the internal pore diameter.

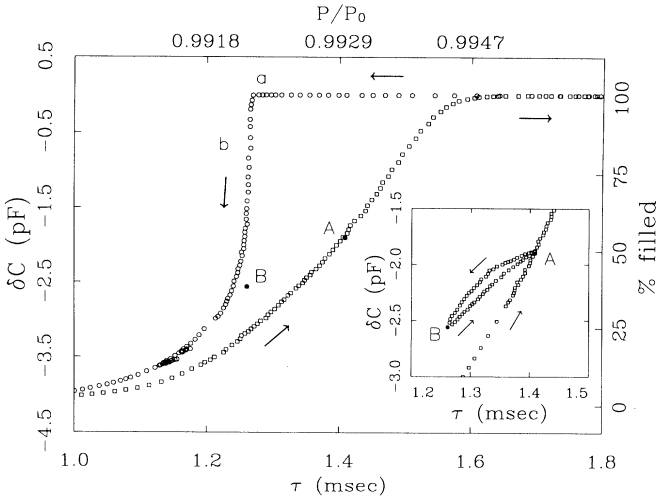

FIG. 1. Capillary condensation hysteresis loop for nominal 2000 Å pore diameter Nuclepore at $T = 1.52$ K. $\delta C = C - C_{\text{full}}$ is the change in the capacitance of the Nuclepore-helium sample from the completely capillary condensed value of the capacitance. τ is the time of flight of third sound and serves as an *in situ* monitor of the chemical potential. P/P_0 is the ratio of the vapor pressure to the saturated vapor pressure at $T = 1.52$ K deduced [4] from third sound. The arrows denote the trajectory followed around the loop for a complete filling-emptying cycle. Points labeled "*a*" and "*b*" are referenced in the text. Inset: An example of a subloop: adding helium along the global hysteresis loop to point A, removing helium to point B, and adding helium again to point A. Return point memory is demonstrated.

Of interest here is substructure which is present in cases where a more complicated evolution [7] of the chemical potential is followed. For example, consider the inset to Fig. 1. For the experiment represented here, at point A on the global hysteresis loop helium is withdrawn from the sample cell causing the capacitance signal to follow the upper trajectory A-B. Then, following arrival at point B, helium is again admitted to the cell and the lower trajectory B-A is followed. The point A reproduces precisely as the trajectory rejoins the global loop; the system demonstrates *return point memory* [8]. This can be understood by consideration of the fact that the Nuclepore sample consists of a huge number of pores with a small but finite distribution of pore sizes. As the chemical potential initially reaches point A, a subset γ of these pores has capillary condensed. As helium is withdrawn, some of these γ pores drain and when we reach point B, a subset of the γ pores, ξ, has opened *in a particular order*. As helium is again added, this same fraction ξ of the pores fills, but in a different order; thus, the open loop. When A is reached, the complete fraction ξ has filled, thus restoring the filled fraction γ, and point A reproduces exactly. This is analogous to the *return point memory* behavior seen in, for example, ferromagnetic systems, and often described by the model originally due to Preisach [9].

In the Preisach model, a hysteretic system is assumed to be made up of *independent* domains (here, pores), each of which can be switched "on" (filled) at particular values of the chemical potential, α_i, and "off" (drained) at a different value of the chemical potential, β_i; $\alpha_i > \beta_i$. A real system consists of a number N of such domains (pores), each characterized by a point (α_i, β_i) in α-β space. As the chemical potential is increased various pores fill. A reduction in chemical potential drains a subset of these pores; subsequent increase in the chemical potential to the original value restores the original set of filled pores; thus demonstrating return point memory.

The data display a number of other interesting features. For example, consider Fig. 2 in which we display several subloops [Figs. 2(a) and 2(b)] taken between two sets of chemical potential end points. The subloop and sub-subloop shapes appear nearly identical. Two subloops, taken between the same chemical potential end points, will be congruent if the system under study consists of independent (and therefore noninteracting) elements and is thus fully describable by the Preisach model. Close examination of the data shows that we have near but not precise congruence; the different subloops appear slightly rotated (Fig. 2, inset) relative to one another [10]. The Nuclepore system shows deviations from the Preisach model. Therefore, the material cannot consist of completely independent pores; the pores must interact.

More powerful evidence for the presence of interactions and a failure of the Preisach model can be seen in Fig. 3, where we show data for two nested subloops initiated

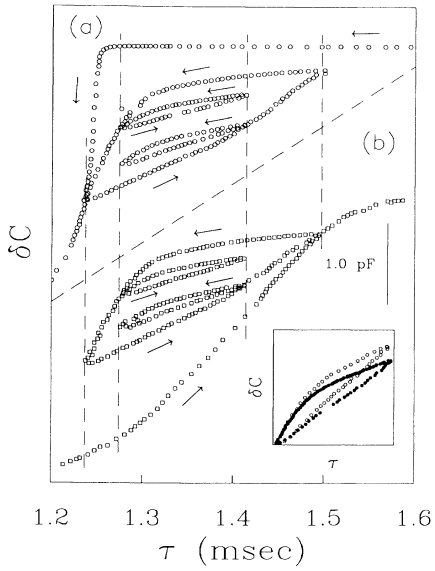

FIG. 2. Example of a more complicated set of trajectories. Note the presence of return point memory in all six subloops and the near congruence of the two large loops and the four smaller loops. The filling (b) and draining (a) segments of the main hysteresis loop have been displaced vertically for clarity. The inset shows more clearly the lack of precise congruence for the case of the top two sub-subloops; the vertical scale has been expanded to better illustrate the effect.

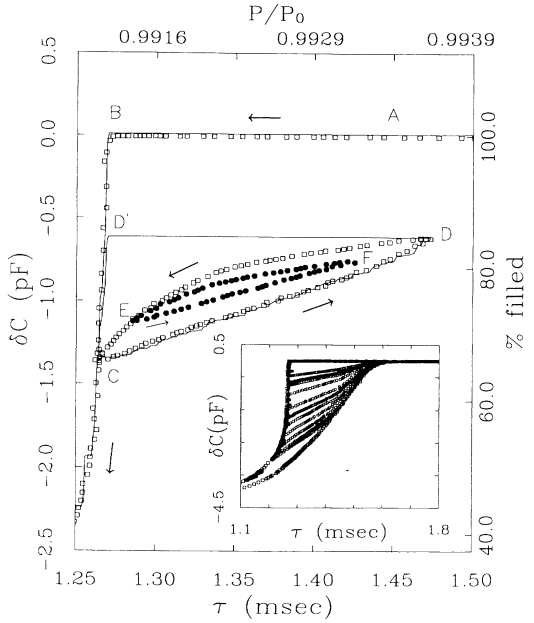

FIG. 3. Example of subloop structure measured (symbols) and predicted (solid curves) from first order reversal curves (inset) and the Preisach model [9]. The letters denote trajectories discussed in the text.

from point C on the global draining curve. For a system obeying the Preisach model, first order reversal curves [for example, filling trajectories (Fig. 3, inset) which begin along the path B-C in Fig. 3] yield information which can be translated into a measure of $\mu(\alpha_i,\beta_i)$, the distribution of switching points in α-β space for the ensemble of individual hysteretic elements. Knowledge of this distribution function allows one to predict the exact Preisach behavior of interior subloops. We have measured a number of such reversal curves (Fig. 3, inset) for the Nuclepore system. Each point on a reversal curve determines the proper weighting for a small rectangle (α_j,β_i) to $(\alpha_{j+1},\beta_{i+1})$ in α-β space. Using this calculated $\mu(\alpha,\beta)$, a double integral [11] over the appropriate surface, which is determined by the evolution of the chemical potential, predicts [9] the set of resulting hysteresis loops. The lack of success of such a prediction [12] is shown by the solid line in Fig. 3.

To gain a perspective on the failure of the independent domain model to adequately predict our results, we consider next a mechanism for interaction effects among the pores which is not present in the Preisach model. The Preisach model predicts that subloops should begin to drain at the chemical potential value at which the global hysteresis loop begins to drain (point B, Fig. 3). Thus, the Preisach model predicts trajectories A-B and D-D' to be horizontal; pores full at A or D are predicted to remain so on withdrawal of helium until the chemical potential associated with point B is reached. A-B is horizontal; D-E is not. Along trajectory A-B, *all* pores are filled; draining may only commence from pore openings at the surface and the largest available β_i is not reached until point B. At point D, however, some pores are open because they drained during the trajectory B-C. These open pores intersect others which are still filled. Consider one such open pore that intersects another that is still closed (except perhaps for the intersection region). Since the diameter of the pore is larger inside the material than it is on the surface, this closed pore has associated with it at the intersection *new* coordinates β_i' due to the presence of new draining points of the closed pore which are now present inside the Nuclepore (rather than on the surface). These new β_i are now available to participate so as to create the trajectory D-E. These interior pore openings are not present to participate along the trajectory A-B since all the pores are filled along that trajectory and the internal intersections do not present a fluid-vapor interface as they do along the trajectory D-E. The exposed internal pore openings also cause subloop E-F-E to be open. We expect that many porous capillary condensed systems display this internal pore-opening effect. Because of the structure of the Nuclepore, pore blocking, assumed to be an important effect in many capillary condensed systems, may not be an important effect here.

We believe that for Nuclepore pore intersections result in interactions. For hysteretic systems interactions are predicted [13] to cause avalanche effects; here the draining event associated with one pore is expected to induce further draining of the system. In an effort to observe the

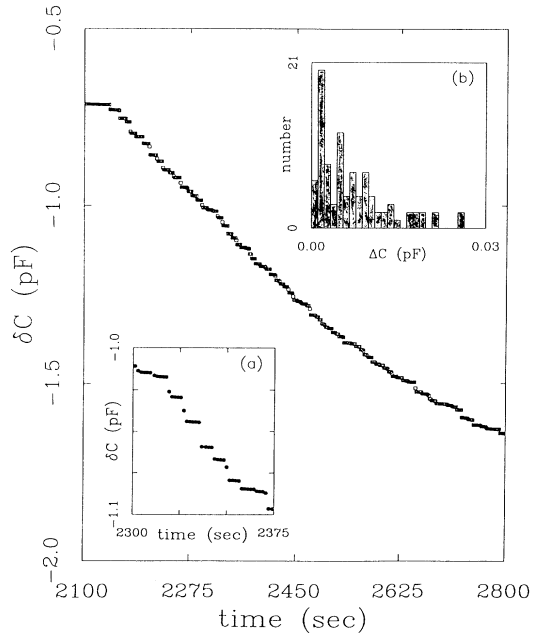

FIG. 4. An example of avalanche events observed on slow withdrawal of helium from the cell beginning near the point labeled "*b*" in Fig. 1. Shown is the capacitance vs time for a typical withdrawal. Insets show (a) an expanded view of the step structure and (b) a histogram of number of avalanches vs avalanche size for the draining data shown.

discreteness of such behavior, we prepare the system by first filling the pores and then bringing the system to point "*a*" shown in Fig. 1. Then, capacitance vs time is monitored during the gradual withdrawal of helium from the cell. An example of the observation of avalanche behavior near point "*b*" (Fig. 1) is shown in Fig. 4, where avalanche events of size ΔC, in the range $0.0005\ \text{pF} < \Delta C < 0.03\ \text{pF}$ which, assuming only pores are involved, corresponds to a fraction $f = n/N$ of the pores in the sample $0.0001 < f < 0.007$ draining as an avalanche, are seen. The largest avalanche we have observed in any of our experiments involves $\sim 2.6 \times 10^7$ pores, $f \sim 0.026$. In a perfect interacting system, the avalanche staircase would be exactly reproducible. This is not the case here, although repetitions of the experiment result in histograms of avalanche number vs size [inset, Fig. 4(b)] and distributions of avalanche size vs percent filled which are very similar. The absence of exact staircase reproducibility is presumably due to temperature fluctuations (measured to be no larger than ± 0.5 mK), or perhaps to pumping rate variations or vibrations. Analysis of the available data in terms of occurrence vs avalanche size shows an apparent power law behavior over a limited range of avalanche size. Substantial improvements in the apparatus may allow more precise power law and frequency analysis of such avalanche data in the future, including an accurate determination of the power law exponent.

In summary, we have demonstrated memory effects and the near congruence of hysteretic subloops in a system which demonstrates capillary condensation. The system displays a number of the gross features expected based on a model of hysteretic behavior originally proposed by Preisach to describe hysteresis and magnetic systems. Deviations from the predictions of the simple model are observed and proposed to have their origin in the interactions due to the microstructure [14] of the porous system. These interactions lead to avalanche events which are observed.

We acknowledge informative discussions with K. Dahmen, R. A. Guyer, S. Karth, and J. Krumhansl. This work was supported by the National Science Foundation through DMR 91-22348. One of us (R.B.H.) acknowledges support from the J. S. Guggenheim Memorial Foundation.

[1] Nuclepore is a trademark of Costar, Cambridge, MA.
[2] D. S. Cannell and F. Rondelez, Macromolecules **13**, 1599 (1980); D. Bragg, Costar (private communication).
[3] D. T. Smith, K. M. Godshalk, and R. B. Hallock, Phys. Rev. B **36**, 202 (1987); K. M. Godshalk and R. B. Hallock, Phys. Rev. B **36**, 8294 (1987).
[4] See, for example, S. J. Putterman, *Superfluid Hydrodynamics* (North-Holland, Amsterdam, 1974).
[5] Rapid addition or subtraction of helium from the cell causes relaxation phenomena to occur.
[6] W. F. Saam and M. W. Cole, Phys. Rev. B **11**, 1086 (1975).
[7] M. P. Lilly and R. B. Hallock, in Proceedings of the 20th International Conference on Low Temperature Physics [Physica (Amsterdam) (to be published)].
[8] See, for example, J. A. Barker, D. E. Schreiber, B. G. Huth, and D. H. Everett, Proc. R. Soc. London A **386**, 251 (1983); D. J. Holocomb, J. Geophys. Res. **86**, 6235 (1981); J. Ortin, J. Appl. Phys. **71**, 1454 (1992).
[9] F. Preisach, Z. Phys. **94**, 277 (1935).
[10] This effect is not due to the rate of change of the amount of helium in the experimental cell.
[11] Mayergoyz [I. D. Mayergoyz, J. Appl. Phys. **57**, 3803 (1985)] has restated the Preisach model so that the reversal curves will directly yield the hysteresis loops without the need to explicitly calculate $\mu(\alpha,\beta)$ or perform double integrals. The Mayergoyz formulation is equivalent to the approach we have taken.
[12] The experiments have an addition element; pores, in addition to being either empty or full, can be decorated by a superfluid film of variable thickness (up to $\sim 1\%$ of the volume of the pore). This film growth is a modest effect and is unable to explain a number of the deviations seen in our work.
[13] J. D. Sethna, K. Dahmin, S. Kartha, J. A. Krumhansl, B. W. Roberts, and J. D. Shore, Phys. Rev. Lett. **70**, 3347 (1993).
[14] At the conclusion of this work we became aware of the work of Page *et al.* [J. H. Page, J. Liu, B. Abeles, H. W. Deckman, and D. A. Weitz, Phys. Rev. Lett. **71**, 1216 (1993)] for the case of Vycor which also notes the importance of internal structure; in their case pore blocking was a major effect.